Atmos. Chem. Phys. Discuss., 6, 12929–12965, 2006
www.atmos-chem-phys-discuss.net/6/12929/2006/

Atmospheric Chemistry and Physics Discussions

Observations of total peroxy nitrates and aldehydes: measurement interpretation and inference of OH radical concentrations

P. A. Cleary[1,*], P. J. Wooldridge[1], D. B. Millet[2,], R. C. Cohen[2], M. McKay[2,4], and A. H. Goldstein[1,3,4]**

[1]Dept. of Chemistry, University of California, Berkeley, Berkeley, CA 94720, USA
[2]Dept. of Environmental Science, Policy and Management, University of California, Berkeley, Berkeley, CA 94720, USA
[3]Dept. of Earth and Planetary Science, Univ. of California, Berkeley, Berkeley, CA 94720, USA
[4]Environment Technologies Division, Lawrence Berkeley National Laboratory, Berkeley, CA 94720, USA
[*]now at: Department of Chemistry, University of Pennsylvania, 231 S. 34th St, Philadelphia, PA 19104, USA
[**]now at: Department of Earth and Planetary Sciences, Harvard University, Cambridge, MA 02138, USA

Received: 30 October 2006 – Accepted: 30 November 2006 – Published: 12 December 2006

Correspondence to: R. C. Cohen (cohen@cchem.berkeley.edu)

Abstract

We describe measurements of total peroxy nitrates (ΣPNs), NO_2, O_3 and several aldehydes at Granite Bay, California, during the Chemistry and Transport of the Sacramento Urban Plume (CATSUP) campaign, from 19 July–16 September 2001. We observed a strong photochemically driven variation of ΣPNs during the day with the median of 1.2 ppb at noon. Acetaldehyde, pentanal, hexanal and methacrolein had median abundances in the daytime of 1.2 ppb, 0.093 ppb, 0.14 ppb, and 0.27 ppb, respectively. We compare a steady state and a time dependent calculations of the dependence of ΣPNs on aldehydes, OH, NO and NO_2 showing that the steady state calculations of are be accurate to ±30% between 10:00 a.m. and 06:00. We use the steady state calculation to investigate the composition of ΣPNs and the concentration of OH at Granite Bay. We find that PN molecules that have never been observed before make up an unreasonably large fraction of the ΣPNs unless we assume that there exists a PAN source that is much larger than the acetaldehyde source. We calculate that OH at the site varied between 1 and 6×10^6 molecules cm^{-3} at noon during the 8 weeks of the experiment.

1 Introduction

Peroxyacyl nitrates (or peroxycarboxylic nitric anhydrides) are a class of atmospheric reactive nitrogen ($NO_y \equiv$ NO + NO_2 + peroxy nitrates + alkyl and multifunctional nitrates + HONO + HNO_3 + NO_3 + 2 × N_2O_5) produced by photochemical reactions of aldehydes and photolysis of ketones, such as acetone and methyl glyoxal (Blitz et al., 2004; Roberts et al., 2002; Romero et al., 2005). Peroxyacetyl nitrate, PAN, the most abundant and widely studied peroxyacyl nitrate, is produced through the reaction of acetaldehyde with OH, (R1) producing peroxyacyl radical ($CH_3C(O)O_2$, or PA) followed by the association of PA with NO_2 (R2). Other sources of PA, such as methyl glyoxal photolysis, may be important, especially where isoprene is the predominant reactive volatile organic compound (VOC) (Roberts et al., 2001). Loss of PAN occurs primarily

by the sequential processes of thermal decomposition to regenerate PA (R-2) followed by reaction of PA with NO (R3).

$$\text{acetaldehyde} + OH(+O_2) \rightarrow PA + H_2O \quad \text{(R1)}$$

$$PA + NO_2 \rightarrow PAN \quad \text{(R2)}$$

$$PAN \rightarrow PA + NO_2 \quad \text{(R-2)}$$

$$PA + NO \rightarrow \text{products} \quad \text{(R3)}$$

$$PAN + OH \rightarrow \text{products} \quad \text{(R4)}$$

The reaction of PAN with OH (R4) is slow Talukdar et al., 1995, however this sink of PNs may be important for other PN species, such as MPAN. Figure 1 summarizes the processes represented by (R1)–(R4). The thermal decomposition of PAN (R-2) has a steep temperature dependence. PAN has a lifetime to thermal decomposition of hours or less in the lower troposphere (T>287 K) and of months in the mid- to high latitude free troposphere (Temp<263 K). PAN that is created in situ or transported to the upper troposphere from a source region near the surface can be transported globally Beine et al., 1996; Singh and Hanst, 1981. When the air containing PAN warms, NO_2 is released; thus PAN serves as a vehicle for global scale redistribution of NO_x ($NO_x \equiv$ NO + NO_2). Peroxyacyl nitrates are also a well known component of urban photochemistry (Corsmeier et al., 2002b; Rappengluck et al., 2003; Singh, 1987; Stephens et al., 1956). PAN is often observed to be correlated with O_3 (Corsmeier et al., 2002a; Gaffney et al., 1999; Gaffney et al., 2002; Penkett and Brice, 1986; Rappengluck et al., 2000; Rubio et al., 2004) and the ratios of different PANs have been used to assess the relative contributions of anthropogenic and biogenic sources of O_3 (Roberts et al., 2001; Williams et al., 1997).

In addition to PAN, other peroxy nitrates are formed following OH-initiated hydrogen abstraction of larger aldehydes. Simultaneous measurements of the ambient

concentrations of the aldehyde – peroxyacyl nitrate pairs, propanal-peroxyproprionic nitric anhydride (PPN) (Roberts et al., 2001, 2003), acrolein-peroxyacrylic nitric anhydride (APAN) (Roberts et al., 2003), and methacrolein-MPAN (Roberts et al., 2001, 2003) have been described. The peroxyacyl nitrates derived from isobutanal: peroxyisobutyric nitric anhydride (PiBN) (Roberts et al., 2002, 2003), n-butanal: peroxy-n-butyric nitric anhydride (PnBN) (Gaffney et al., 1999; Glavas and Moschonas, 2001) and benzaldehyde: peroxybenzoic nitric anhydride (PBzN) (Atkinson and Lloyd, 1984) have also been identified in the atmosphere. Many other PN compounds have been observed in the laboratory (Hurst-Bowman et al., 2003; Noziere and Barnes, 1998; Sehested et al., 1998; Tyndall et al., 2001; Wallington et al., 1995) and based on these laboratory and field measurements, it is reasonable to assume that virtually every aldehyde observed in the atmosphere should have a corresponding peroxyacyl nitrate. Glavas and Moshonas (Glavas and Moschonas, 2001) have argued that the relative ratios of peroxy nitrates can be deduced from the ratios of parent aldehydes. Roberts et al. (2001, 2003) use a sequential reaction model (Reactions 1–4 and their analogues as applied to each PN/aldehyde pair) to explain the correlations between the observed ratios of PPN/propanal, PAN/acetaldehyde, MPAN/methacrolein and APAN/acrolein (Roberts et al., 2001, 2003). In their analyses, Roberts et al. (2001, 2003) attribute the variability PN/aldehyde ratios to plume age and assume that the observations represent oxidation of an isolated plume downwind of a localized source of aldehydes. They show this model does a reasonable job at representing the correlations between different ratios of PN/aldehyde pairs.

In this paper, we describe simultaneous measurements of total peroxy nitrates (ΣPNs), aldehydes, NO_2 and O_3 at the eastern edge of the suburbs of Sacramento, CA as a part of the CATSUP (Chemistry and Transport of the Sacramento Urban Plume) experiment. We take a different point of view from the papers of Roberts et al. (2001, 2003) and assume that PNs in the urban boundary layer do not result from emission at a point source but rather are continually affected by emissions of their aldehyde precursors. We compare time dependent and steady state calculations for PNs showing

that PNs are in approximate steady state with their source molecules. We then use the steady state calculation to investigate the partitioning of ΣPNs among a variety of individual peroxy nitrates and to investigate the concentration of OH at the Granite Bay site.

2 Experimental

Observations of NO_2, ΣPNs, total alkyl nitrates (ΣANs), HNO_3, O_3, VOC, and meteorological variables were collected from 19 July–16 September 2001 on the property of Eureka Union School District in Granite Bay, CA (38 E 44.23′ 121 E 12.01′, 277 m above sea level). This site is located 30 km north-east of Sacramento, CA, at the eastern edge of the suburban region and between two major highways: Interstate 80, 8 km to the north and Highway 50, 13 km to the south. The instruments were housed in a temperature-controlled trailer with inlets mounted on a rooftop tower 7 m above the ground, (1–2 m above the trailer).The site and instruments are described in detail in Cleary et al. (Cleary et al., 2005) and only a brief description is included here.

Briefly, wind patterns observed at the site were quite regular, at speeds of 2–2.4 m/s from the southwest (directly from Sacramento) during the afternoon (12:00–17:00 h) and from the southeast at 1.6 m/s (downslope from the Sierra Nevada) at night (20:00–06:00 h). On most days, the wind direction rotated smoothly and continuously from southeasterlies to southwesterlies between the hours of 06:00–12:00 h and then rotated back between 17:00 and 20:00. On a typical day, the air parcels observed at Granite Bay at noon had arrived at the Sacramento urban core from the South and then turned toward Granite Bay traveling over the entire length of the Sacramento metropolitan region. Temperatures (mean $\pm 1\sigma$) at Granite Bay during the campaign were 16 (±2.4) ˚C at 05:00 rising to 33 (±3.6) ˚C at 16:00. Skies were clear on all but two days of the campaign, as determined from observations of photosynthetically active radiation. O_3 was measured with a Dasibi 1008 ultraviolet photometric ozone analyzer.

NO_2, ΣPNs, ΣANs and HNO_3 were measured using a two-channel thermal-dissociation laser induced fluorescence (TD-LIF) instrument (Day et al., 2002). Briefly, an ambient sample flows rapidly through two ovens where dissociation of NO_z (NO_z ≡HNO_3 + ΣANs+ΣPNs) species to NO_2 occurs. Three different temperatures are used: 180˚C, 350˚C and 550˚C, to observe the three distinct classes of NO_z: ΣPNs, ΣANs and HNO_3. The ΣPNs measurement includes PAN, PPN, MPAN, PiBN, PBN and any other peroxy nitrate present in the atmosphere. N_2O_5 dissociates at this temperature; however, for the inlet configuration we used at Granite Bay, it is likely N_2O_5 was converted to HNO_3 on the inlet surfaces prior to the dissociation region. The NO_2 signal is the sum of the NO_2 contained in all compounds that dissociate at or below the oven temperature, and the difference between the NO_2 observed in two separate channels at adjacent temperature set points is associated with a specific class of compounds. For these measurements NO_2 was measured using a pulsed dye laser with time gated detection (Thornton et al., 2000).

We measured NO_2, ΣPNs, ΣANs, and HNO_3 by sequentially adjusting the temperatures of each oven so the pair of ovens remained only one class of NO_y species apart. The measurements were made on a 4-h repeating cycle. Each time an oven set point was raised, it was pre-programmed to overshoot the set point for a few seconds in order to remove compounds adsorbed to the walls. ΣANs were measured for 75 min each cycle, ΣPNs and NO_2 for 40 min each cycle, and HNO_3 for 80 min each cycle, with the remaining time used for measuring zeros, calibrating, and obtaining other diagnostics. During the last six days of the campaign, 11 September–16 September, ΣPNs and NO_2 were measured continuously.

The accuracy for each class of NO_y compound is 15%. Comparison of LIF with other NO_2 measurements indicates the LIF measurements of NO_2 are within 5% of other NO_2 measurements (Thornton et al., 2003). The NO_2 signals observed by TD-LIF are adjusted to account for small (5%) effects of secondary chemistry within our inlet (Rosen et al., 2004). The most important effects are associated with reactions of RO_2 (e.g. PA) radicals and O_3 with NO. The extent of these interferences depends on

the inlet configuration. Over the last few years, we have used 3 different configurations. The configuration used for the Granite Bay experiments was identical to that used in Houston (Rosen, 2004), except that the machined PFA Teflon inlet tip piece was replaced with standard molded fittings for better HNO_3 transmission. This inlet was a 2-channel version of the one described in detail by Day et al. (2002). A key feature was the insertion of pressure-reducing orifices between the heated tubes and the 15 to 20 m long PFA Teflon tubes leading to the instrument housed at the base of the tower. Laboratory experiments confirm that interferences in this configuration are small and that our corrections accurately accounted for their effects. Comparison of ΣPNs to the sum of individual PAN compounds using this inlet and two other inlet configurations during experiments in Houston, TX (Rosen, 2004), from the DC-8 aircraft, from the NCAR C-130 and at a surface site in Nova Scotia have shown that ΣPNs are usually within 15% of the sum of PAN, PPN and MPAN (Wooldridge et al., 2006[1]). The largest differences we have ever observed, as much as 30% ($\Sigma PNs > \Sigma PN_i$), were observed when sampling ambient air during the PAN Intercomparison Experiment in Boulder, CO during summer 2005. During this experiment agreement between ΣPN and specific PN measurements was within 10% for test samples of specific compounds including PAN and PPN (Tyndall et al., 2005). However, the poor agreement when sampling ambient air was shown to result from a large interference in the ΣPN measurements that was proportional to the product of NO with O_3. Laboratory experiments confirm that the configuration used for the PIE experiments, which omitted the pressure reduction orifices at the back of the heaters in order to keep the pressure at nearly ambient up to the expansion nozzles for the supersonic jets (based on the design outlined by Cleary et al., 2002), resulted in much higher interferences than other configurations because of the longer residence times and higher pressures within 20 m of tubing connecting the heated inlet and the instrument. The inlet configuration used for the Granite Bay

[1]Woolridge, P. J., Perring, A. E., and Cohen, R. C.:Total Peroxy Nitrates: the Thermal Dissociation-Laser Induced Fluorescence Technique and Comparisons to Speciated PAN Measurements, in preparation, 2006.

experiments had a more rapid pressure drop and thus has much smaller interferences, ones that we believe are accurately accounted for in the analysis.

Most of the potential systematic error in the individual classes observed by TD-LIF are correlated, in the sense that if ΣPNs are too high by 5% then likely so are NO_2, ΣANs and HNO_3. In contrast, ratios of the different classes will be more accurate because these systematic effects will cancel.

We did not measure NO or NO_y directly. We calculate NO using the photostationary state equation:

$$[NO]_{ss} = \frac{j_{NO_2}[NO_2]}{k_{NO+O_3}[O_3] + k_{HO_2+NO}[HO_2 + RO_2]} \quad (1)$$

Noontime HO_2+RO_2 concentrations are calculated to be 0.050 ppb. The photolysis rate of NO_2 was estimated by scaling the J-values obtained from the TUV model (UCAR, 2002) for 11 August 2001, using total ozone column of 299 DU, as measured by TOMS (McPeters, 2001) to the observed PAR. ΣNO_{yi} is calculated as the sum of NO_{ss}, NO_2, ΣPNs, ΣANs, and HNO_3.

Volatile organic compounds, including aldehydes, were measured hourly with a fully automated, in situ, two-channel gas chromatograph/mass selective detector/flame ionization detector (GC/MSD/FID) system. This system has been described in detail elsewhere (Millet et al., 2005). Briefly, the FID channel was configured for analysis of C_3-C_6 alkanes, alkenes, and alkynes, and the MSD channel for analysis of a range of other VOC, including aromatic, oxygenated and halogenated compounds. For 36 min out of every hour, two subsample flows (15 ml/min) were drawn from the main sample line (4 liters/min) and passed through a preconditioning trap for the removal of water (–25°C cold trap). Carbon dioxide and ozone were scrubbed from the FID channel subsample (Ascarite II), and ozone was removed from the MSD channel subsample (KI impregnated glass wool). Preconcentration was accomplished using a combination of thermoelectric cooling (–15°C) and adsorbent trapping. Samples were injected into the GC by rapidly heating the trap assemblies to 200°C. The instrument was calibrated several

times daily by dynamic dilution (factor of 1000) of low ppm level standards (Scott Marin Inc., and Apel-Riemer Environmental Inc.) into zero air. Zero air was analyzed daily to check for blank problems and contamination for all measured compounds. Final data represent samples collected from 15 to 51 min of each hour (a 36 min integral).

The ΣPN and NO_2 measurements were put on a common time base with the VOC measurements by averaging over the 36 min of the VOC sampling. Data are included in this analysis if a minimum of 15 min of ΣPNs and NO_2 were obtained during the 36 min VOC sampling window.

3 Observations

Measurements of ΣPNs and NO_2 from 19 July–16 September 2001 are shown in Fig. 2. ΣPNs ranged from 0 to 0.080 ppb at night and had a midday peak that typically occurred between noon and 01:00 p.m. ranging from 0.5–2.5 ppb, with a median of 1.2 ppb. The average daytime (08:00–20:00 h) mixing ratio of ΣPNs was 0.910 ppbv. NO_2 peaked during both the morning and evening rush hours with mean concentrations of 8 and 10 ppb, respectively. Typical noontime concentrations of NO_2 were 4.5 ppb. At noon, ΣPNs are typically 10% of ΣNO_{yi}, and they range from 10–30% of NO_z. These observations of ΣPN mixing ratios are within the typical range of peroxy-nitrates measured at other locations. For example, at the University of California Blodgett Forest Research Center, 5 h downwind of the Granite Bay site, summertime ΣPN measurements peak later in the day (08:00 p.m.) at around 0.550 ppb, are 10–20% of ΣNO_{yi} and 15–25% of NO_z (Day et al., 2003). Roberts et al. (2002) report the sum of 3 PNs: PAN, PPN and MPAN, observed outside of Nashville in June 1999, had an average daytime mixing ratio of 1.14 ppb (10% of NO_y). At La Porte, Texas during August-September 2000, Roberts et al. (2001) report the sum of 5 different PNs, PAN, PPN, MPAN, PiBN and APAN was on average 1.18 ppb, an amount we calculate was 8% of NO_y and 17% of NO_z (NO_y-NO_x) at that site.

The aldehyde observations are shown in Fig. 3. Acetaldehyde is the most abundant

aldehyde, with concentrations ranging 0.5 to 3 ppb. Except for methacrolein, the aldehydes reached a maximum at night (when the boundary layer is thinnest) suggesting that in addition to photochemical production, direct emissions and/or NO_3 chemistry affect the abundance of aldehydes at this site. Acetaldehyde was generally constant in the morning, then decreased in the early afternoon, rising in the evening to its nighttime maximum. However, several different daytime patterns were observed as shown in Fig. 4a, which shows acetaldehyde and ΣPN observations from 11–16 September 2001. Nearly constant daytime acetaldehyde was observed on 12 and 16 September; a morning increase and afternoon decrease were observed on 13 and 15 September ; and a sharp midday decrease was observed on 14 September. On 11 September, the acetaldehyde mixing ratio increased throughout the day. Pentanal and hexanal have similar diurnal patterns to acetaldehyde, although they both show patterns of decreasing midday concentration more frequently than acetaldehyde. Methacrolein generally increased in the morning and peaked in the afternoon, and was strongly correlated to isoprene mixing ratios. Median daytime observations of acetaldehyde, pentanal, hexanal and methacrolein were 1.2 ppb, 0.093 ppb, 0.14 ppb, and 0.27 ppb, respectively.

Our observed mixing ratios of aldehydes are in the range of those reported at two other urban sites, as shown in Table 1. Grossman et al. (2003) measured C_2-C_{10} aldehydes and methacrolein in July 1998 near Berlin and report the higher n-aldehydes (C_7-C_{10}) had a diurnal pattern with maxima at 10:00 a.m. and minima at midnight. McClenny et al. (1998) report n-aldehydes at Nashville are strongly correlated with each other, and exhibit a diurnal cycle with minima in the early evening and maxima at noon. Wedel et al. (1998) report C_5-C_9 n-aldehydes in rural north-eastern Germany, during August, 1994 and describe night-time maxima in aldehydes. Concentrations of all aldehydes were much lower at this rural site. Grossman et al. (2003) also report that typical maxima were 2–5 times the minima for all aldehydes observed. These observations indicate that the aldehydes we were able to observe are not a complete set. Measurements have shown that there are significant aldehyde emissions from a variety of plant species (Vuorinen et al., 2005; Wildt et al., 2003) and that aldehydes

are produced as a result of ozonolysis reactions with fatty acids. Nonanal has received special attention because its production is particularly favorable (Hung et al., 2005; Thornberry and Abbatt, 2004). Ambient mixing ratios for propanal, butanal and hexanal have been reported to be higher than those of pentanal; while mixing ratios of heptanal and octanal are lower than pentanal. Nonanal has been observed at mixing ratios approximately double those of pentanal.

4 Steady state calculation of peroxy nitrates

ΣPNs, the measurement of total peroxy nitrates, are a new measurement (Day et al., 2002), not previously analyzed in detail. To evaluate the contributions of individual PNs (denoted PN_i) to ΣPNs we note that when temperatures and OH concentrations are high, individual PNs are approximately in steady state with their acetaldehyde sources (R1) and their sink through the peroxy radical (PA_i) + NO Reaction (R3). PN_i and PA_i are in rapid steady state with a lifetime on the order of minutes for typical surface conditions at Granite Bay in summer, at a daytime mean of 297 K. The steady state condition for the sum of a PN_i and PA_i will be satisfied when the lifetime of PN_{Ti} (PN_{Ti}=PA_i+PN_i) is of order a few hours or less and the concentration of the acetaldehyde precursor is nearly constant on that timescale. For example, the lifetime of [PAN+PA] with respect to loss to R3 is on the order of 40 min at 298 K using rate coefficients outlined in Table 2 at typical noontime values of NO and NO_2 at Granite Bay. The lifetimes of other PNs are similar or shorter in cases where the reaction with OH is rapid. Thus, at temperatures greater than 298 K, each PN_i approaches a steady state with its aldehyde source in about an hour. However, the lifetime of acetaldehyde with respect to loss to OH at noon (298 K, OH = 6×10^6 molecules/cm^3) is about 3 h. If there were no sources of aldehydes, PNs might not reach a steady state when OH mixing ratios are at their peak, because of the rapidly decreasing aldehyde concentrations. However, as discussed above, aldehydes exhibit a range of diurnal patterns and the aldehydes are often observed to have nearly constant mixng ratios or to be decreasing more slowly

than the lifetime of 3 h during the day. Thus, PN_{Ti} likely achieves near steady-state conditions.

Steady state equations for PA_i and the (PN_{Ti})/aldehyde$_i$ ratio derived from Reactions (1)–(4) are:

$$[PA_i]_{ss} = \frac{k_{1aldehyde_i}[OH] * [aldehyde_i] + k_{-2}[PN_i]}{k_2[NO_2] + k_3[NO]} \quad (2)$$

$$\frac{[PN_T]_i}{[aldehyde]_i} = \frac{k_{1aldehyde_i} * \beta * [OH]}{k_{-2} * (1-\beta) + k_4[OH]} \text{ where } \beta = \frac{1}{\frac{k_3[NO]}{k_2[NO_2]} + 1} \quad (3)$$

These equations assume each PN has a single aldehyde source and that the only important sink of PNs is reaction of PA with NO. For the conditions at Granite Bay, we calculate that PA radicals make up less than 1% of HO_2 + RO_2 and the loss rate for any peroxy-radical to reaction with NO is about 300 times faster than peroxy-radical self reactions.

In order to evaluate the accuracy of the steady state approximation represented by Eqs. (2) and (3), we solved the differential equation (Eq. 4) describing PAN mixing ratios over the course of a day by numerical integration:

$$\frac{d(PAN)}{d(t)} = \beta(t) * k_1[\text{acetaldehyde}(t)][OH] - k_{-2} * (1-\beta(t)) * [PAN(t)]. \quad (4)$$

We compare the solution of the time dependent integration to the instantaneous steady state solution using 4 different models of the production/emission rates for acetaldehyde. The four scenarios were: A) acetaldehyde production equal to loss (P_{acet}=L_{acet}), B) acetaldehyde production equal to zero (P_{acet}=0), C) acetaldehyde production equal to 1.5 times loss (P_{acet}=1.5L_{acet}) and D) P_{acet}=1.5L_{acet} from sunrise to noon, and P_{acet}=2/3L_{acet} from noon to sunset. Acetaldehyde loss (L_{acet}) was determined by its reaction rate with the OH field defined above. The acetaldehyde concentrations produced in these scenarios are shown in Fig. 5b. Scenario A is a close match to the observations on 12 September 2001. Scenario D produces acetaldehyde concentrations

similar to that observed on 13 September 2001. Scenarios B and C represent limiting cases that describe behavior of acetaldehyde outside the range of the observations and thus put useful bounds on the comparison of the time dependent and steady state calculations.

The calculations were initialized using 0.300 ppb for [PAN] and 1.0 ppb for [acetaldehyde]. These are typical values at sunrise. We used as input the median diurnal cycles of the ratio [NO]/[NO_2], temperature, and an estimate for OH of 1.4×10^7 molecules cm^{-3} at noon (based on the results of Dillon et al. , 2002). The temporal variation in OH was estimated by scaling to PAR. These parameters are shown in Fig. 5.

Figures 6a and b, respectively, show the steady state and time dependent calculations of PAN for scenarios A and D. Figure 6c shows the ratio of the steady state (SS) to the time dependent (TD) calculations of PAN versus time of day for all 4 scenarios. After an initial spin up time of about two hours, the SS calculation is within ±30% of the TD calculation through the remainder of the day for scenarios A, C and D. For scenario A when acetaldehyde concentrations are constant, the steady state calculation agrees with the TD calculation to within ±10%. For scenario B, where the production of acetaldehyde is zero, the acetaldehyde concentration is changing most rapidly compared to the PAN lifetime. As a result, the time dependent calculation has higher PN concentrations than steady state. Even in this scenario the time dependent calculation differs from the steady state approximation by only 60% (SS/TD=0.4). For scenario C, the net acetaldehyde lifetime is comparable to the PAN lifetime and the steady state calculation predicts 40% more PAN than the time dependent calculation before 11:00 h. The two calculations for scenario C converge to within 25% at noon. The sign of the SS/TD ratio reflects that production of acetaldehyde is larger than losses in scenario C. Scenario D represents a situation such as on 13 September where there is net production of acetaldehyde in the morning but a decrease during the afternoon. This scenario combines the effects seen in scenarios B and C. The steady state calculation overestimates PAN in the morning, crosses through a point where the two calculations agree at about noon before underestimating PAN for the remainder of the afternoon.

We tested whether the comparison of time-dependent and steady state calculations had a strong sensitivity to the assumed OH. Using a more than ten-fold decrease in OH, 1×10^6 at noon, the differences between the steady state and time dependent calculations decreased slightly for scenarios B, C, and D at all times of the day. Steady-state and time dependent calculations using the lower OH agreed less well during the rush hour when the NO/NO_2 ratio is highest for scenario A.

Most of the observations have similar diurnal patterns to scenarios A or D, and we interpret the comparisons presented in this section to indicate that the steady state approximation for PN to aldehyde ratios is accurate to 30% or better outside of the rush hour periods.

5 Partitioning of ΣPNs and estimates of OH

We calculate ΣPNs as the sum of steady state expressions (EQN 3) for each individual peroxy nitrate:

$$\Sigma PNs = \frac{\beta * k_{1i}[OH] * [acet]}{k_{-2}(1-\beta)+k_{4i}[OH]} + \frac{\beta * \alpha_i * k_{1i}[OH] * [MACR]}{k_{-2}(1-\beta)+k_{4i}[OH]} + \frac{\beta * \alpha_i * k_{1i}[OH] * [ptnl]}{k_{-2}(1-\beta)+k_{4i}[OH]} + \frac{\beta * \alpha_{i*} k_{1i}[OH] * [hxnl]}{k_{-2}(1-\beta)+k_{4i}[OH]} + \ldots \quad (5)$$

The reaction rate for each aldehyde with OH (k_{1i}), each PN_i with OH (k_{4i}) and the branching ratio of aldehydic abstraction (α_i) by OH are specific to each PN_i/aldehyde$_i$ pair. For example, MPAN has a significant loss to reaction with OH, producing products that are not ΣPNs (Orlando et al., 2002). The reactions of other PNs with OH are slow, but the magnitudes may increase with carbon number (Jenkin et al., 1997). The reactions of each peroxy-radical with NO_2 and NO (rate constants k_2 and k_3) are estimated to be the same for all peroxyacyl radicals. The dissociation of each PN back to NO_2 (k_{-2}) is also estimated to be the same as that measured for PAN (Atkinson et al., 1997; Atkinson et al., 2004). The unique solution to Eq. (5) results in determination of the OH concentration and the concentrations for individual peroxy nitrates for each point in the data set. In our tests of the accuracy of the steady-state model we calculated PAN from aldehydes and an assumed profile of OH, the accuracy estimate of 30% for that

relationship also applies to calculations of OH using measured ΣPNs and aldehydes, if the assumption that the ΣPNs and aldehydes are in steady-state holds and if the aldehyde sources of PA_i represented in the model are a complete set.

We solve Eq. (5) for three models: A) using the observed aldehydes and constraining the relationship of PPN to PAN, B) adding to model A an estimate of the concentration for a broader range of aldehydes and C) adding to model B an additional source of PAN. One of the more abundant and well-studied PNs is PPN. However, we do not have a measurement of propanal, the aldehyde precursor to PPN. At inland sites in California, the PPN/PAN ratio has been observed to be 0.15 with little variation (Grosjean et al., 2002, and references therein). Thus we fix the PPN to PAN ratio at 0.15 and adjust the propanal concentration accordingly in all three models.

In model B we estimate the mixing ratio of other aldehydes based on prior observations at other urban locations (Grossman et al., 2003; McClenny et al., 1998; Wedel et al., 1998; Hurst-Bowman et al., 2003). We include isobutanal, along with C_4, C_7, C_8, and C_9 n-aldehydes. C_4, C_7 and C_8 aldehydes are estimated to occur at the same mixing ratio as pentanal and nonanal is estimated to be twice as abundant as pentanal. Table 3 lists the rate constants (298K) for the reaction of C_2-C_9 aldehydes with OH along with the average noontime concentrations that we observed or that we estimate. The branching ratio between aldehyde-H abstraction, which leads to PN formation, and alkyl-H abstraction, which we assume does not, increases with the carbon chain length of the n-aldehydes. For propanal, the ratio of OH abstraction at the aldehydic hydrogen to the alkyl hydrocarbons is estimated to be 95% and for butanal 90% (Jenkin, et al., 1997) The ratio of aldehyde-H abstraction to alkyl abstraction for nonanal was calculated to be 50% by Hurst-Bowman et al. (2003). As an estimate for other species we smoothly connect the butanal and nonanal points, decreasing the reaction at the aldehydic hydrogen by 8% per carbon (82% for pentanal, 74% for hexanal, 66% for heptanal and 58% for octanal). For methacrolein, observations indicate 45% of OH reactions abstract the aldehydic hydrogen (Orlando et al., 1999).

In model C, we include an added source of PA radicals contributing to the formation of PAN. Roberts et al. (2001) suggest there is a large source of PA radicals other than acetaldehyde based on their observations in Nashville, TN, an urban area where isoprene dominates local photochemistry. One suggestion for this source is methylglyoxal (Romero et al., 2005), which is a product of isoprene oxidation and thus likely abundant both in Granite Bay, CA and in Nashville, TN. Based on the calculations by Roberts et al., the missing source of PA could be 2 to 3 times larger than the PA source from acetaldehyde. For scenario C, we add an additional source of PA radicals that fixes PAN at 70% of ΣPNs.

The calculated partitioning of peroxy-nitrates using the inputs described above are shown in Table 4. PAN is calculated to be the largest portion of ΣPNs, 65% for model A, 50% in model B, and constrained to be 70% for model C. For model A, PPN, C_5PAN, C_6PAN and MPAN are 9.8, 7.7, 11 and 6.3% of ΣPNs, respectively. In model B, PNs that have never been observed in the atmosphere are estimated to contribute about 1/3 of the total peroxy nitrates, with C_9PAN and C_6PAN the most abundant of these, each at 8.5% of ΣPNs. Comparisons of ΣPNs with measurements of individual PNs suggest that the 1/3 contribution for previously unmeasured PNs is too large (Roberts et al., 2003; Rosen, 2004; Wooldridge et al., 2006[1]). The contribution of PAN to ΣPNs observed during our previous measurements was never less than 70% and was typically 80%. Thus model C represents a situation that is consistent with the lower end of the prior observations of the PAN/ΣPNs ratio. We found it necessary to insert a source of PA radicals that is 3 times the acetaldehyde source alone in order to increase the PAN fraction of the ΣPNs. In our calculation we have implemented this increase by simply increasing the concentration of acetaldehyde. This has the effect of reducing the calculated OH substantially because of the inverse relationship between the OH that is calculated by rearranging Eqs. (3) and (5) and aldehyde sources of PNs. If the sole source were instead photolysis and reaction of OH with methylglyoxal, with a noon photolysis rate coefficient of 2×10^{-4} s^{-1}, and a rate constant for reaction of OH of 1.7×10^{-11} cm^3-$molecule^{-1}$-s^{-1} about 0.5 ppb of methylglyoxal would be required. This

would result in a much higher calculated concentration of OH (about a factor of 2), but not so high as to be inconsistent with other estimates. However this concentration of methylglyoxal is likely larger than what is present as the average observed daytime concentrations of methacrolein and methyl vinyl ketone which are thought to be the primary precursors to methylglyoxal are only 0.6 and 0.3 ppb, respectively. We conclude that a source of PA radicals in addition to methylglyoxal must be present in Sacramento to explain the PAN:ΣPN ratio.

The calculated partitioning of ΣPNs varies little over the course of the day because the ratio of aldehydes varies little, although some of the PNs may have much lower mixing ratios in the background atmosphere than PAN and may therefore be more affected by mixing, especially early in the day. The peak abundance of each peroxy nitrate and its ratio to PAN from model C are very similar to other measurements. For example, Roberts et al. (1998, 2001, 2002) report daytime MPAN to PAN ratios ranging from 3–9% during experiments Nashville (1994, 1995, 1999) and in Houston (2000), with average concentrations for MPAN of 0.048 ppb (Nashville, 1994), 0.037 ppb (Nashville, 1995), 0.084 ppb (Nashville, 1999) and 0.030 ppb (Houston, 2000). Our estimates of the same quantities are 6% and 0.030 ppb using model C. Models A and B both result in MPAN to PAN ratios of 10–11%, higher than any of these prior measurements. Roberts et al. (2001) report average daytime PiBN/PAN ratios of ∼2% at La Porte, TX. Our estimate of the PiBN/PAN ratio from model C is 2% and for model B it is 5%, double that observed in La Porte, TX. The distribution of PNs in model C has a contribution of 15% from PNs that have never previously been measured in ambient samples. We believe this is too high. The most likely reason is that ΣPNs are slightly out of steady state, although the possibilities that the higher PNs have much faster atmospheric removal processes or that PAN sources other than acetaldehyde are even larger than we speculated in model C should also be explored.

The calculated OH (model C) has a strong diurnal cycle with midday peaks 1–3 h after local noon ranging from $1–6\times10^6$ molecules/cm^3 on different days (Figs. 4 and 7). The median results are 2.8×10^6 and 4.6×10^6 molecules cm^{-3} at 12:00 h and 14:00 h,

respectively. The inverse relation between modeled PN sources (Eqs. 3 and 5) results in OH calculated using model A that is 250% larger and model B that 100% larger than that calculated with model C. If some large fraction of the PAN production is photolysis of an aldehyde instead of oxidation by OH, then the OH could be as high as that indicated by model B. Figure 4b shows the calculated OH (Model C) on 11 September–16 September. Notice that for very different ΣPN and acetaldehyde concentrations, similar OH profiles are derived. For example, on both 11 September and 13 September, the modeled OH peaks at 2×10^6 molecules cm^{-3} while acetaldehyde and ΣPN measurements peak at midday on 13 September at concentrations roughly twice that of 11 September. Given the approximations that are used to calculate OH, these specific values should be interpreted with caution until a more extensive comparison of this method for inferring OH and direct OH measurements can be made.

The OH we calculate is lower than the values derived from oxidation/dilution analyses of observations downwind of Granite Bay within the Sacramento plume by Dillon et al. (2002); Schade et al. (2002) and Dreyfus et al. (2002). Lower OH at Granite Bay than in the average over the Sacramento plume is expected because the Granite Bay site is NO_x saturated and OH should increase as NO_x decreases downwind (Murphy et al., 2006a, b). It is also possible that we underestimate the OH because of treating the additional PAN source as acetaldehyde rather than assuming it is photolytic. The diurnal profile of the calculated OH during the entire campaign is shown in Fig. 7. The black squares represent the mean values and the solid lines $\pm1\sigma$ for each 1-h bin u. We infer a median OH of 2.8×10^6 molecules cm^{-3} at noon and of 4.7×10^6 molecules cm^{-3} at 14:00 h. This asymmetry about noon is consistent with recent measurements of OH by Martinez et al. (2002); Ren et al. (2003) who report maxima at ∼02:00 p.m. Similar noontime OH concentrations have been reported for Los Angeles $3–6\times10^6$ molecules cm^{-3} (George et al., 1999) and Munich, Germany $4.5–7.4\times10^6$ molecules cm^{-3} (Handisides et al., 2003).

6 Conclusions

We describe observations of ΣPNs, aldehydes, NO_2 and O_3 at Granite Bay, CA from 19 July–16 September 2001. The observations are used to characterize the partitioning of ΣPNs and to demonstrate the possibility of determing the mixing ratio of OH if the sources of PNs were accurately known. We calculate that PAN is likely 65% of ΣPNs if acetaldehyde is the only PAN source, a value too low to be consistent with prior measurements, suggesting a prominent role for another source of PA radicals. Constraining PAN to be 70% of ΣPNs and PPN to be 15% of PAN, we estimate MPAN is 3% of ΣPNs, PiBn is 1% and that the sum of C_5 and larger PNs that have not previously been observed outside the laboratory to be 15% of ΣPNs. This value for the fraction of ΣPNs that are species that have never before been observed in the atmosphere is likely too high. We suspect that this is due to PNs being out of steady state with their sources. We also calculate a diurnal profile of OH at the site that is in reasonable correspondence with direct observations at other locations and derive a median OH of 2.6×10^6 molecules cm^{-3} at noon.

We have compared a steady state and time dependent calculation for PNs showing that the steady state calculation is accurate to 30%. This implies a relatively rapid interconversion between NO_x and ΣPNs in urban plumes, such that ΣPNs do not represent a terminal sink of NO_x. The quantities NO_x, NO_y and NO_z have been widely interpreted based on the assumption that NO_z is quite slowly (if at all) returned to the NO_x pool. Our results suggest that rethinking the use of these quantities is necessary. We calculate that peroxy nitrates are usually in steady state with NO_2 on a time scale of 40 min. In the urban plume described in this manuscript, ΣPNs range from 1/4 to about 1/2 of NO_2 during midday. This short lifetime and the high relative concentrations of peroxy nitrates compared to NO_x imply that the PNs component of NO_z can buffer NO_x concentrations in the planetary boundary layer. Thus as the Sacramento plume (and by analogy many other urban plumes) is transported downwind PNs decompose keeping NO_x higher than would be the case if PNs were a permanent NO_x sink. As

an alternative to the usual definitions of NO_x and NO_z we suggest that NO_x+PNs and HNO_3+ANs (or NO_y-NO_x-PNs) be used in analyses of the correlations of O_3 and NO_x in warm urban plumes.

Acknowledgements. We gratefully acknowledge the U.S. Department of Energy support for measurements under contract AC03-76SF0009 and National Science Foundation support for analysis under grant ATM-0138669. D. Millet also acknowledges a DOE GCEP fellowship for funding. We are grateful to the Eureka Union School District for the use of the measurement site.

References

Atkinson, R. and Lloyd, A. C.: Evaluation of Kinetic and Mechanistic Data For Modeling of Photochemical Smog, J. Phys. Chem. Ref. Data, 13, 315–444, 1984.

Atkinson, R.: Gas-Phase Tropospheric Chemistry of Organic-Compounds, J. Phys. Chem. Ref. Data, 2, 1–216, 1994.

Atkinson, R., Baulch, D. L., Cox, R. A., Hampson, R. F., Kerr, J. A., Rossi, M. J., and Troe, J.: Evaluated kinetic and photochemical data for atmospheric chemistry: Supplement VI – IUPAC subcommittee on gas kinetic data evaluation for atmospheric chemistry, J. Phys. Chem. Ref. Data, 26, 1329–1499, 1997.

Atkinson, R., Baulch, D. L., Cox, R. A., Crowley, J. N., Hampson, R. F., Hynes, R. G., Jenkin, M. E., Rossi, M. J., and Troe, J.: Evaluated kinetic and photochemical data for atmospheric chemistry: Volume I – gas phase reactions of O_x, HO_x, NO_x and SO_x species, Atmos. Chem. Phys., 4, 1461–1738, 2004, http://www.atmos-chem-phys.net/4/1461/2004/.

Beine, H. J., Jaffe, D. A., Blake, D. R., Atlas, E., and Harris, J.: Measurements of PAN, alkyl nitrates, ozone, and hydrocarbons during spring in interior Alaska, J. Geophys. Res.-Atmos., 101, 12 613–12 619, 1996.

Blitz, M. A., Heard, D. E., Pilling, M. J., Arnold, S. R., and Chipperfield, M. P.: Pressure and temperature-dependent quantum yields for the photodissociation of acetone between 279 and 327.5 nm, Geophys. Res. Lett., 31, L06111, doi:10.1029/2003GL018793, 2004.

Cleary, P. A., Wooldridge, P. J., and Cohen, R. C.: Laser-induced fluorescence detection of

atmospheric NO_2 with a commercial diode laser and a supersonic expansion, Appl. Opt., 41, 6950–6956, 2002.

Cleary, P. A., Murphy, J. G., Wooldridge, P. J., Day, D. A., Millet, D. B., McKay, M., Goldstein, A. H., and Cohen, R. C.: Observations of total alkyl nitrates within the Sacramento Urban Plume, Atmos. Chem. Phys. Discuss., 5, 4801–4843, 2005, http://www.atmos-chem-phys-discuss.net/5/4801/2005/.

Corsmeier, U., Kalthoff, N., Vogel, B., Hammer, M. U., Fiedler, F., Kottmeier, C., Volz-Thomas, A., Konrad, S., Glaser, K., Neininger, B., Lehning, M., Jaeschke, W., Memmesheimer, M., Rappengluck, B., and Jakobi, G.: Ozone and PAN formation inside and outside of the Berlin plume – Process analysis and numerical process simulation, J. Atmos. Chem., 42, 289–321, 2002a.

Corsmeier, U., Kalthoff, N., Vogel, B., Hammer, M. U., Fiedler, F., Kottmeier, C., Volz-Thomas, A., Konrad, S., Glaser, K., Neininger, B., Lehning, M., Jaeschke, W., Memmesheimer, M., Rappenglueck, B., and Jakobi, G.: Ozone and PAN Formation Inside and Outside of the Berlin Plume – Process Analysis and Numerical Process Simulation, J. Atmos. Chem., 42, 289–321, 2002b.

Day, D. A., Wooldridge, P. J., Dillon, M. B., Thornton, J. A., and Cohen, R. C.: A thermal dissociation laser-induced fluorescence instrument for in situ detection of NO_2, peroxy nitrates, alkyl nitrates, and HNO_3, J. Geophys. Res.-Atmos., 107, 4046, doi:10.1029/2001JD000779, 2002.

Day, D. A., Dillon, M. B., Wooldridge, P. J., Thornton, J. A., Rosen, R. S., Wood, E. C., and Cohen, R. C.: On alkyl nitrates, O_3, and the "missing NO_y", J. Geophys. Res.-Atmos., 108, 4501, doi:10.1029/2003JD003685, 2003.

Dillon, M. B., Lamanna, M. S., Schade, G. W., Goldstein, A. H., and Cohen, R. C.: Chemical evolution of the Sacramento urban plume: Transport and oxidation, J. Geophys. Res.-Atmos., 107, 4045, doi:10.1029/2001JD000969, 2002.

Dreyfus, G. B., Schade, G. W., and Goldstein, A. H.: Observational constraints on the contribution of isoprene oxidation to ozone production on the western slope of the Sierra Nevada, California, J. Geophys. Res., 107, 4365, doi:10.1029/2001JD001490, 2002.

Gaffney, J. S., Marley, N. A., Cunningham, M. M., and Doskey, P. V.: Measurements of peroxyacyl nitrates (PANS) in Mexico City: implications for megacity air quality impacts on regional scales, Atmos. Environ., 33, 5003–5012, 1999.

Gaffney, J. S., Marley, N. A., Drayton, P. J., Doskey, P. V., Kotamarthi, V. R., Cunningham, M. M.,

Baird, J. C., Dintaman, J., and Hart, H. L.: Field observations of regional and urban impacts on NO_2, ozone, UVB, and nitrate radical production rates in the Phoenix air basin, Atmos. Environ., 36, 825–833, 2002.

George, L. A., Hard, T. M., and O'Brien, R. J.: Measurement of free radicals OH and HO2 in Los Angeles smog, J. Geophys. Res., [Atmospheres], 104, 11 643–11 655, 1999.

Glavas, S. and Moschonas, N.: Determination of PAN, PPN, PnBN and selected pentyl nitrates in Athens, Greece, Atmos. Environ., 35, 5467–5475, 2001.

Grosjean, E., Grosjean, D., Woodhouse, L. F., and Yang, Y. J.: Peroxyacetyl nitrate and peroxypropionyl nitrate in Porto Alegre, Brazil, Atmos. Environ., 36, 2405–2419, 2002.

Grossmann, D., Moortgat, G. K., Kibler, M., Schlomski, S., Bachmann, K., Alicke, B., Geyer, A., Platt, U., Hammer, M. U., Vogel, B., Mihelcic, D., Hofzumahaus, A., Holland, F., and Volz-Thomas, A.: Hydrogen peroxide, organic peroxides, carbonyl compounds, and organic acids measured at Pabstthum during BERLIOZ, J. Geophys. Res.-Atmos., 108, 8250, doi:10.1029/2001JD001096, 2003.

Handisides, G. M., Plass-Duelmer, C., Gilge, S., Bingemer, H., and Berresheim, H.: Hohenpeissenberg Photochemical Experiment (HOPE 2000): measurements and photostationary state calculations of OH and peroxy radicals, Atmos. Chem. Phys., 3, 1565–1588, 2003, http://www.atmos-chem-phys.net/3/1565/2003/.

Hung, H. M., Katrib, Y., and Martin, S. T.: Products and mechanisms of the reaction of oleic acid with ozone and nitrate radical, J. Phys. Chem. A, 109, 4517–4530, 2005.

Hurst-Bowman, J., Basket, D. J., and Shepson, P. B.: Atmospheric chemistry of nonanal, Environ. Sci. Technol., 38, 2218–2225, 2003.

Jenkin, M. E., Saunders, S. M., and Pilling, M. J.: The tropospheric degradation of volatile organic compounds: A protocol for mechanism development, Atmos. Environ., 31, 81–104, 1997.

Kwok, E. S. C. and Atkinson, R.: Estimation of Hydroxyl Radical Reaction-Rate Constants For Gas- Phase Organic-Compounds Using a Structure-Reactivity Relationship – an Update, Atmos. Environ., 29, 1685–1695, 1995.

Martinez, M., Harder, H., Brune, W., Di Carlo, P., Williams, E., Hereid, D., Jobson, T., Kuster, W., Roberts, J., Trainer, M., Fehsenfeld, F. C., Hall, S., Shetter, R., Apel, E., Reimer, D., and Geyer, A.: The behavior of the hydroxyl and hydroperoxyl radicals during TexAQS2000, paper presented at AGU Fall Meeting, EOS Transactions, San Francisco, CA, USA, 2002.

McClenny, W. A., Daughtrey, E. H., Adams, J. R., Oliver, K. D., and Kronmiller, K. G.: Volatile

organic compound concentration patterns at the New Hendersonville monitoring site in the 1995 Southern Oxidants Study in the Nashville, Tennessee, area, J. Geophys. Res.-Atmos., 103, 22 509–22 518, 1998.

McPeters, R. D.: TOMS, edited by NASA, 2001.

Millet, D. B., Donahue, N. M., Pandis, S. N., Polidori, A., Stanier, C. O., Turpin, B. J., and Goldstein, A. H.: Atmospheric volatile organic compound measurements during the Pittsburgh Air Quality Study: Results, interpretation, and quantification of primary and secondary contributions, J. Geophys. Res.-Atmos., 110, D07S07, doi:10.1029/2004JD004601, 2005.

Murphy, J. G., Day, D. A., Cleary, P. A., Wooldridge, P. J., Millet, D. B., Goldstein, A. H., and Cohen, R. C.: The weekend effect within and downwind of Sacramento: Part 1. Observations of ozone, nitrogen oxides, and VOC reactivity, Atmos. Chem. Phys. Discuss., 6, 11 427–11 464, 2006a.

Murphy, J. G., Day, D. A., Cleary, P. A., Wooldridge, P. J., Millet, D. B., Goldstein, A. H., and Cohen, R. C.: The weekend effect within and downwind of Sacramento: Part 2. Observational evidence for chemical and dynamical contributions, Atmos. Chem. Phys. Discuss. 6, 11 971–12 019, 2006b.

Noziere, B. and Barnes, I.: Evidence for formation of a PAN analogue of pinonic structure and investigation of its thermal stability, J. Geophys. Res.-Atmos., 103, 25 587–25 597, 1998.

Orlando, J. J., Tyndall, G. S., and Paulson, S. E.: Mechanism of the OH-initiated oxidation of methacrolein, Geophys. Res. Lett., 26, 2191–2194, 1999.

Orlando, J. J., Tyndall, G. S., Bertman, S. B., Chen, W. C., and Burkholder, J. B.: Rate coefficient for the reaction of OH with $CH_2=C(CH_3)C(O)OONO_2$ (MPAN), Atmos. Environ., 36, 1895–1900, 2002.

Penkett, S. A. and Brice, K. A.: The spring maximum in photo-oxidants in the Northern Hemisphere troposphere, Nature (London, United Kingdom), 319, 655–657, 1986.

Rappengluck, B., Oyola, P., Olaeta, I., and Fabian, P.: The evolution of photochemical smog in the Metropolitan Area of Santiago de Chile, J. Appl. Meteorol., 39, 275–290, 2000.

Rappengluck, B., Melas, D., and Fabian, P.: Evidence of the impact of urban plumes on remote sites in the Eastern Mediterranean, Atmos. Environ., 37, 1853–1864, 2003.

Ren, X. R., Harder, H., Martinez, M., Lesher, R. L., Oliger, A., Shirley, T., Adams, J., Simpas, J. B., and Brune, W. H.: HO_x concentrations and OH reactivity observations in New York City during PMTACS-NY2001, Atmos. Environ., 37, 3627–3637, 2003.

Roberts, J. M., Williams, J., Baumann, K., Buhr, M. P., Goldan, P. D., Holloway, J., Hubler,

G., Kuster, W. C., McKeen, S. A., Ryerson, T. B., Trainer, M., Williams, E. J., Fehsenfeld, F. C., Bertman, S. B., Nouaime, G., Seaver, C., Grodzinsky, G., Rodgers, M., and Young, V. L.: Measurements of PAN, PPN, and MPAN made during the 1994 and 1995 Nashville Intensives of the Southern Oxidant Study: Implications for regional ozone production from biogenic hydrocarbons, J. Geophys. Res.-Atmos., 103, 22 473–22 490, 1998.

Roberts, J. M., Stroud, C. A., Jobson, B. T., Trainer, M., Hereid, D., Williams, E., Fehsenfeld, F., Brune, W., Martinez, M., and Harder, H.: Application of a sequential reaction model to PANs and aldehyde measurements in two urban areas, Geophys. Res. Lett., 28, 4583–4586, 2001.

Roberts, J. M., Flocke, F., Stroud, C. A., Hereid, D., Williams, E., Fehsenfeld, F., Brune, W., Martinez, M., and Harder, H.: Ground-based measurements of peroxycarboxylic nitric anhydrides (PANs) during the 1999 Southern Oxidants Study Nashville Intensive, J. Geophys. Res.-Atmos., 107, 4554, doi:10.1029/2001JD000947, 2002.

Roberts, J. M., Jobson, B. T., Kuster, W., Goldan, P., Murphy, P., Williams, E., Frost, G., Riemer, D., Apel, E., Stroud, C., Wiedenmyer, C., and Fehsenfeld, F.: An examination of the chemistry of peroxycarboxylic nitric anhydrides and related volatile organic compounds during Texas Air Quality Study 2000 using ground-based measurements, J. Geophys. Res., 108, 4495, doi:10.1029/2003JD003383, 2003.

Romero, M. T. B., Blitz, M. A., Heard, D. E., Pilling, M. J., Price, B., Seakins, P. W., and Wang, L. M.: Photolysis of methylethyl, diethyl and methylvinyl ketones and their role in the atmospheric HOx budget, Faraday Discuss., 130, 73–88, 2005.

Rosen, R. S.: Observations of NO_2, peroxy nitrates, alkyl nitrates, HNO_3, and total NO_y in Houston, TX: implications for O_3 photochemistry, PhD,200, University of California, Berkeley, Berkeley, 2004.

Rosen, R. S., Wood, E. C., Wooldridge, P. J., Thornton, J. A., Day, D. A., Kuster, W., Williams, E. J., Jobson, B. T., and Cohen, R. C.: Observations of total alkyl nitrates during Texas Air Quality Study 2000: Implications for O_3 and alkyl nitrate photochemistry, J. Geophys. Res.-Atmos., 109, D07303, doi:10.1029/2003JD004227, 2004.

Rubio, M. A., Oyola, P., Gramsch, E., Lissi, E., Pizarro, J., and Villena, G.: Ozone and peroxyacetylnitrate in downtown Santiago, Chile, Atmos. Environ., 38, 4931–4939, 2004.

Schade, G. W., Dreyfus, G. B., and Goldstein, A. H.: Atmospheric methyl tertiary butyl ether (MTBE) at a rural mountain site in California, J. Environ. Quality, 31, 1088–1094, 2002.

Sehested, J., Christensen, L. K., Nielsen, O. J., Bilde, M., Wallington, T. J., Schneider, W.

F., Orlando, J. J., and Tyndall, G. S.: Atmospheric chemistry of acetone: Kinetic study of the CH3C(O)CH2O2+NO/NO2 reactions and decomposition of $CH_3C(O)CH_2O_2NO_2$, Int. J. Chem. Kinetics, 30, 475–489, 1998.

Singh, H. B. and Hanst, P. L.: Peroxyacetyl Nitrate (PAN) in the Unpolluted Atmosphere – an Important Reservoir For Nitrogen-Oxides, Geophys. Res. Lett., 8, 941–944, 1981.

Singh, H. B.: Reactive nitrogen in the troposphere, Environ. Sci. Technol., 21, 320–327, 1987.

Stephens, E. R., Hanst, P. L., Doerr, R. C., and Scott, W. E.: Reactions of Nitrogen Dioxide and Organic Compounds in Air, Industrial Eng. Chem., 48, 1498–1504, 1956.

Talukdar, R. K., Burkholder, J. B., Schmoltner, A. M., Roberts, J. M., Wilson, R. R., and Ravishankara, A. R.: Investigation of the Loss Processes For Peroxyacetyl Nitrate in the Atmosphere – UV Photolysis and Reaction With Oh, J. Geophys. Res.-Atmos., 100, 14 163–14 173, 1995.

Thornberry, T. and Abbatt, J. P. D.: Heterogeneous reaction of ozone with liquid unsaturated fatty acids: detailed kinetics and gas-phase product studies, Phys. Chem. Chem. Phys., 6, 84–93, 2004.

Thornton, J. A., Wooldridge, P. J., and Cohen, R. C.: Atmospheric NO_2: In situ laser-induced fluorescence detection at parts per trillion mixing ratios, Analytical Chem., 72, 528–539, 2000.

Thornton, J. A., Wooldridge, P. J., Cohen, R. C., Williams, E. J., Hereid, D., Fehsenfeld, F. C., Stutz, J., and Alicke, B.: Comparisons of in situ and long path measurements of NO_2 in urban plumes, J. Geophys. Res.-Atmos., 108, 4496, doi:10.1029/2003JD003559, 2003.

Tyndall, G. S., Orlando, J. J., Wallington, T. J., and Hurley, M. D.: Products of the chlorine-atom- and hydroxyl-radical-initiated oxidation of CH_3CN, J. Phys. Chem. A, 105, 5380–5384, 2001.

Tyndall, G. S., Apel, E., Williams, E., Flocke, F., Cohen, R. C., Gilge, S., Kim, S., Kim, S., Mills, G., O'Brien, J., Perring, A., Rappenglueck, B., Roberts, J., Schmitt, R., Swanson, A., Tanimoto, H., and Wooldridge, P. J.: PIE 2005: An intercomparison of measurement techniques for peroxynitrates (PANs), paper presented at AGU Fall Meeting, EOS Transactions, San Francisco, 2005.

UCAR: TUV (Total Ultraviolet and Visible radiation model), edited, http://www.acd.ucar.edu/TUV/, 2002.

Vuorinen, T., Nerg, A. M., Vapaavuori, E., and Holopainen, J. K.: Emission of volatile organic compounds from two silver birch (Betula pendula Roth) clones grown under ambient and elevated CO_2 and different O-3 concentrations, Atmos. Environ., 39, 1185–1197, 2005.

Wallington, T. J., Schneider, W. F., Mogelberg, T. E., Nielsen, O. J., and Sehested, J.: Atmospheric Chemistry of FCOx Radicals – Kinetic and Mechanistic Study of the $FCO(O)_2+No_2$ Reaction, Int. J. Chem. Kinetics, 27, 391–402, 1995.

Wedel, A., Muller, K. P., Ratte, M., and Rudolph, J.: Measurements of volatile organic compounds (VOC) during POPCORN 1994: Applying a new on-line GC-MS-technique, J. Atmos. Chem., 31, 73–103, 1998.

Wildt, J., Kobel, K., Schuh-Thomas, G., and Heiden, A. C.: Emissions of oxygenated volatile organic compounds from plants – part II: Emissions of saturated aldehydes, J. Atmos. Chem., 45, 173–196, 2003.

Williams, J., Roberts, J. M., Fehsenfeld, F. C., Bertman, S. B., Buhr, M. P., Goldan, P. D., Hubler, G., Kuster, W. C., Ryerson, T. B., Trainer, M., and Young, V.: Regional ozone from biogenic hydrocarbons deduced from airborne measurements of PAN, PPN, and MPAN, Geophys. Res. Lett., 24, 1099–1102, 1997.

Table 1. Observed aldehydes at Granite Bay in comparison to those made in Berlin (Grossmann et al., 2003), Nashville (McClenny et al., 1998) and rural Germany (Wedel et al., 1998) given as average concentrations.

Aldehyde	this study (ppb)	Berlin Germany[a]	Nashville, TN USA[b]	rural, northwestern Germany[c]
Acetaldehyde	1.20	0.30		
Propanal	0.14[d]	0.20		
Butanal		0.10	0.40	
Pentanal	0.093	0.10	0.22	0.011
Hexanal	0.140	0.15	0.33	0.023
Heptanal		0.07	0.14	0.002
Octanal		0.02	0.27	0.006
Nonanal		0.08	0.52	0.0017
Methacrolein	0.270	0.03		

[a] (Grossmann et al., 2003)
[b] (McClenny et al., 1998)
[c] (Wedel et al., 1998)
[d] estimated

Table 2. Important temperature dependent rate coefficients for PAN and products. All rate coefficients from (Atkinson et al., 1997, 2004).

Reaction	k(T) or k(T,[M])[a]	k (300 K)
PAN → PA + NO_2	$k_0 = 4.9 \times 10^{-3}$ s^{-1}exp (–12100/T) [M] $k_\infty = 5.4 \times 10^{16}$ exp (–13830/T) $F_c = 0.3$ N = 1.41	$6.3\times10^{-4}s^{-1}$
PA + NO_2 → PAN	$k_0 = 2.7 \times 10^{-28}$ $(T/300)^{-7.1}$ [M] $k_\infty = 1.2 \times 10^{-11}$ $(T/300)^{-0.9}$ $F_c = 0.3$ N = 1	8.6×10^{-12} cm^3 $molec^{-1}$ s^{-1}
PA + NO → Products	8.1×10^{-12} exp (270/T)	2.0×10^{-11} cm^3 $molec^{-1}$ s^{-1}

[a] Where $k(M) = \frac{k_0[M]}{1+\frac{k_0[M]}{k_\infty}} * F \log F = \frac{\log F_c}{1+\left(\frac{(\log \frac{k_0[M]}{k_\infty})}{N}\right)^2}$

Table 3. Measured and estimated aldehydes shown with their rate constant with OH, noon lifetime (OH = 1×10^7 molecules cm^{-3}), mean daily concentration and branching ratio to peroxy nitrates.

aldehyde	k^a_{OH} (cm^3 molecule^{-1} s^{-1})	τ^b_{OH} (h)	ave. daytime (ppb)	α
acetaldehyde	1.58×10^{-11}	1.2	1.2	1
propanal	1.96×10^{-11}	1	0.14[c]	0.95[c]
butanal	2.35×10^{-11}	0.8	0.047[c]	0.90[c]
isobutanal	2.63×10^{-11}	0.8	0.047[c]	0.90[c]
pentanal	2.99×10^{-11}	0.6	0.093	0.82[c]
hexanal	3.17×10^{-11}	0.6	0.14	0.74[c]
heptanal	3.03×10^{-11} [d]	0.6	0.093[c]	0.66[c]
octanal	3.17×10^{-11} [d]	0.6	0.093[c]	0.58[c]
nonanal	3.6×10^{-11} [e]	0.5	0.093[c]	0.5
methacrolein	3.35×10^{-11}	0.6	0.27	0.45

[a] Atkinson et al. (1994) unless otherwise stated
[b] [OH] = 1×10^7 molecule cm^{-3}.
[c] estimated
[d] estimated from Kwok et al. (1995)
[e] Hurst-Bowman et al. (2003)

Table 4. Distribution of peroxy nitrates as calculated using aldehydes in Table 3 and Eq. (6). The percent of total peroxy nitrates, the ratio to PAN and the median mixing ratio are given for each model.

PN	% ΣPNs			PN:PAN ratio			daytime average (ppb)			k_{OH}
	A	B	C	A	B	C	A	B	C	$\times10^{-12}$ (cm molecule^{-1} s^{-1})
PAN	65%	50 %	70%	1	1	1	0.58	0.45	0.62	0.03[c]
PPN	9.8%	7.5%	10.5%	0.15	0.15	0.15	0.087	0.067	0.093	N.A.
PnBN	–	2.5%	1.1%	–	0.05	0.02	–	0.022	0.010	4.7[a]
PiBN	–	2.5%	1.1%	–	0.05	0.02	–	0.022	0.010	4.7[a]
C_5PAN	7.7%	5.8%	2.6%	0.12	0.12	0.04	0.069	0.054	0.023	6.9[a]
C_6PAN	11%	8.5%	3.7%	0.17	0.17	0.05	0.099	0.076	0.033	5[a]
C_7PAN	–	4.7%	2.0%	–	0.10	0.03	–	0.045	0.018	8.5[b]
C_8PAN	–	4.4%	1.9%	–	0.09	0.03	–	0.040	0.017	8.5[b]
C_9PAN	–	8.5%	3.7%	–	0.17	0.05	–	0.076	0.033	8.5[b]
MPAN	6.3%	5.5%	3.4%	0.10	0.11	0.06	0.057	0.049	0.030	25.0[d]

[a] Rate coefficients of PNs with OH are based on those reported in the Master Chemical Mechansim where laboratory data is not available.
[b] estimated
[c] (Talukdar et al., 1995)
[d] (Orlandoet al., 2002)
Model A consists of all observed aldehydes and a fixed ratio of PPN:PAN of 0.15.
Model B includes all aldehydes from Model A with additional aldehydes with relative abundances estimated to be similar to those observed at other sites (outlined in Table 3).
Model C included aldehydes from Model B with an additional source of PA radicals.

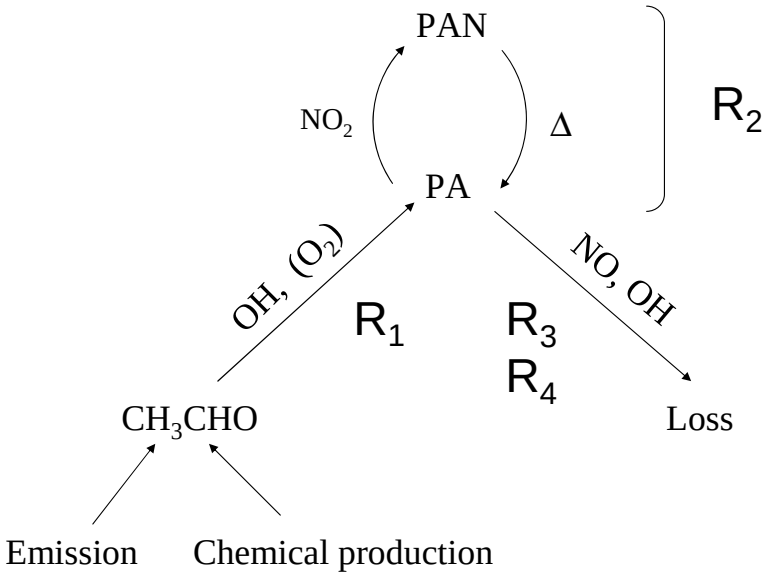

Fig. 1. Diagram of acetaldehyde and PAN photochemistry.

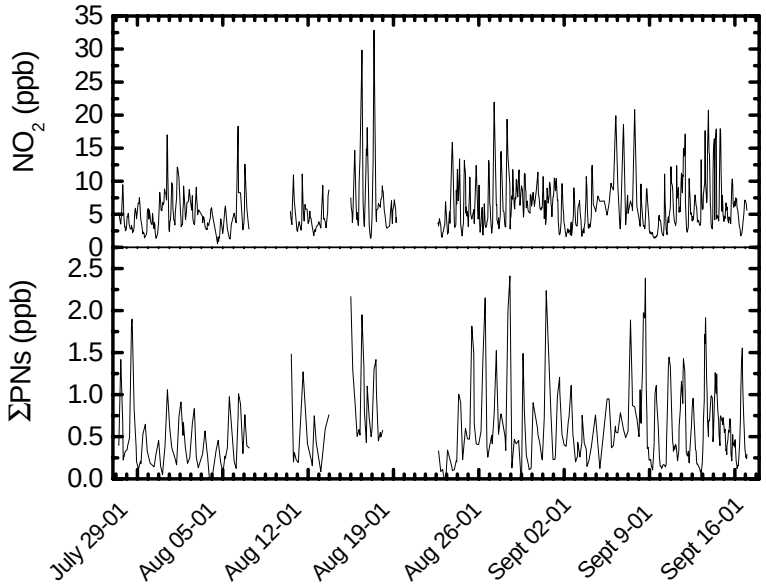

Fig. 2. Measured NO_2 and ΣPNs from 27 July through 16 September 2001. The 10 s data points were placed into 1-h bins corresponding to the VOC time base and the median of each bin is presented here.

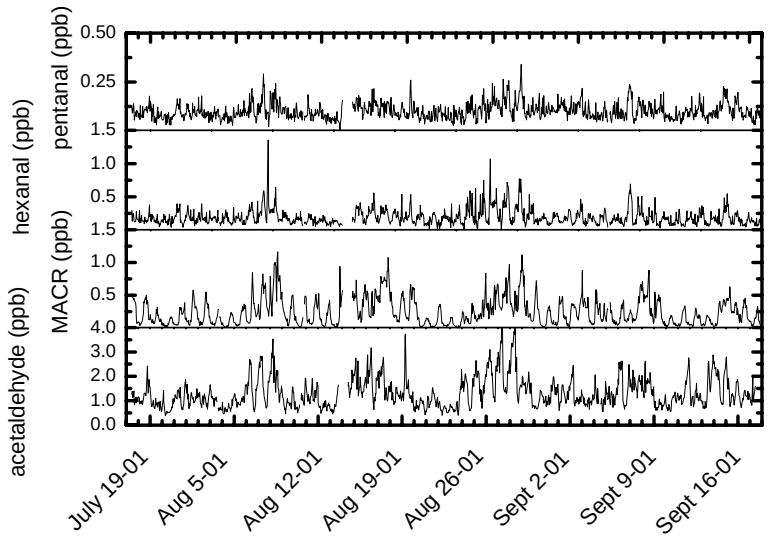

Fig. 3. Hourly measurements of acetaldehyde, methacrolein, pentanal and hexanal from 17 July through 16 September 2001.

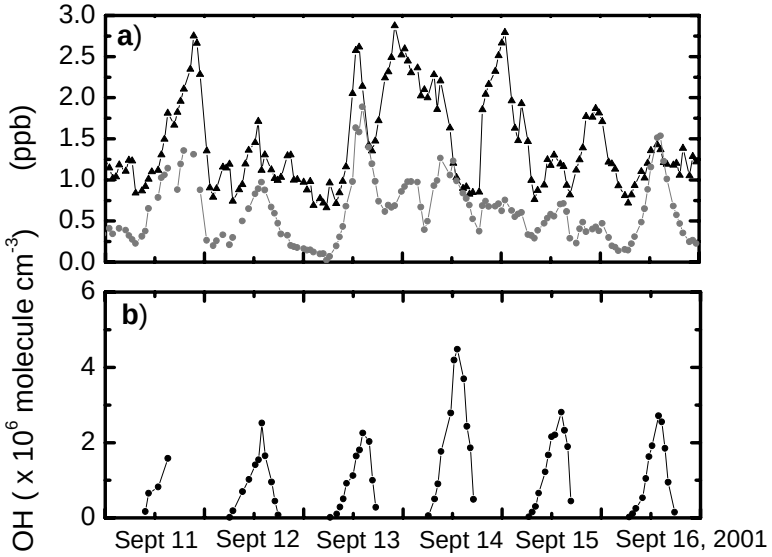

Fig. 4. (a) ΣPN (grey circles) and acetaldehyde (black triangles) measurements are plotted, from 11 September–16 Septembr, when continuous measurements of ΣPNs and NO_2 were made. **(b)** Calculated daytime OH concentrations for the same time period (from Model C).

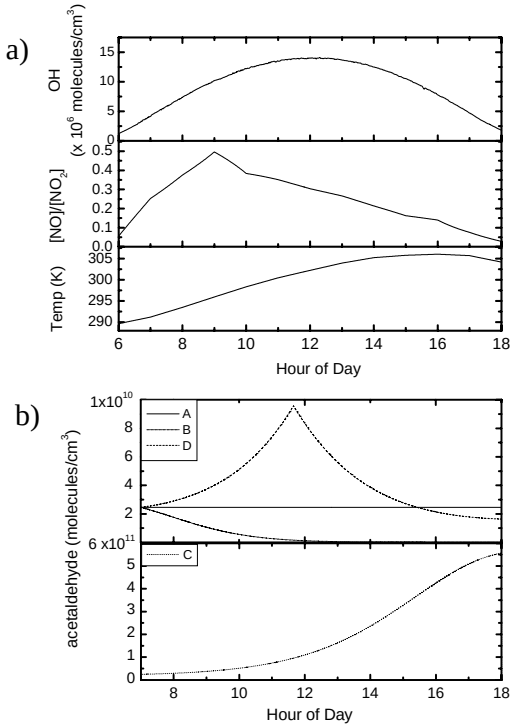

Fig. 5. Time dependent versus steady state model inputs. **(a)** OH (scaled to PAR), the NO/NO_2 ratio, and average observed temperature versus time of day. **(b)** The acetaldehyde concentrations for all scenarios A (constant), B (P_a=0), C (P>L, P=1.25*L) and D (P>L in morning, P<L in evening).

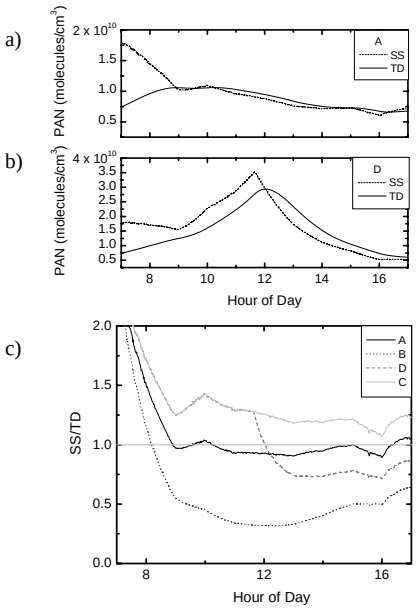

Fig. 6. Steady-state versus time-dependent models of PAN generation. Plot **(a)** shows the diurnal profile of calculated PAN concentrations using scenario D with measured acetaldehyde concentrations as input ($[PAN]_{TD}$= solid line, $[PAN]_{SS}$ = dotted line). Plot **(b)** shows the ratio of $[PAN]_{SS}/[PAN]_{TD}$ versus time of day for the 4 scenarios: A) constant acetaldehyde at 1 ppb, B) production of acetaldehyde = 0, C) $P_a > L_a$, and D) $P_a > L_a$ in the morning and $P_a < L_a$ in the evening , acetaldehyde that is lost to reactions with OH, starting at 1 ppb. Scenario A is the solid line, scenario B is the dot-and-dash dash-dotted line, scenario C is the dotted line and scenario D is dashed line.

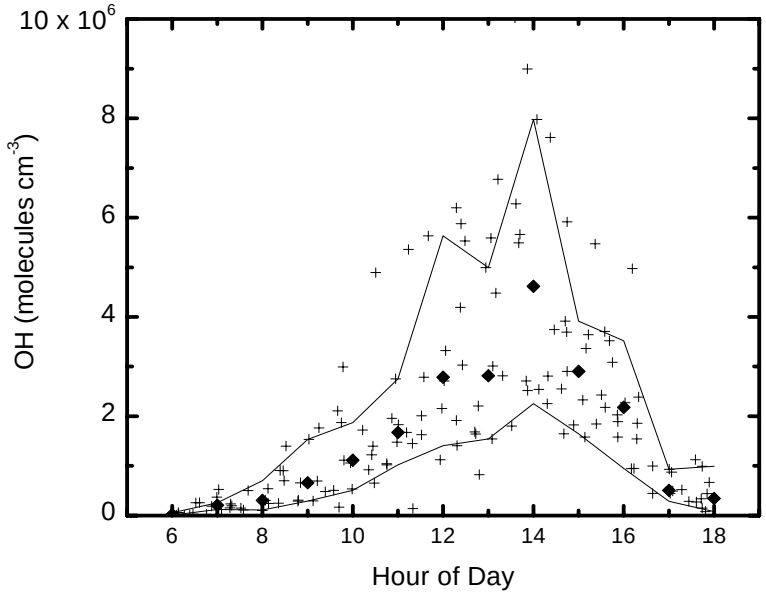

Fig. 7. Diurnal profile of calculated OH concentrations. Median points per 1-h bin are plotted in black squares, $\pm 1\sigma$ from the mean hourly points are plotted in solid line.